ELSEVIER

Available online at www.sciencedirect.com
SCIENCE DIRECT®

Journal of Organometallic Chemistry 689 (2004) 2674–2683

Journal of Organometallic Chemistry

www.elsevier.com/locate/jorganchem

Synthesis, structure and formation pathways of new Fe–S complexes containing $[Fe_2S_2]$-units in different valences, $[Fe_2S_2(CO)_4(PPh_3)_2]$, $[Fe_3S_2(CO)_6(PPh_3)_3]$ and $[Fe_4S_2(CO)_{10}]^{2-}$ and the origin of the $[Fe_2S_2]$-unit in metal–$[Fe_2S_2(CO)_6]$ complexes

Botao Zhuang *, Jun Chen, Lingjie He, Jiutong Chen, Zhangfeng Zhou, Kechen Wu

State Key Laboratory of Structural Chemistry, Fujian Institute of Research on the Structure of Matter,
Chinese Academy of Sciences, Fuzhou, Fujian 350002, China

Received 10 March 2004; accepted 28 May 2004
Available online 3 July 2004

Abstract

Novel Fe–S cluster complexes, $[Fe_2S_2(CO)_4(PPh_3)_2]$ (**1**), $[Fe_3S_2(CO)_6(PPh_3)_3]$ (**2**) and $[Ph_4P]_2[Fe_4S_2(CO)_{10}]$ (**3**) have been synthesized by the reaction of $LiEt_3BH$ with $[Fe_2S_2(CO)_6]$ in the presence of CuCl–PPh_3, $AgNO_3$–PPh_3 and $CuClO_3$–MeCN, respectively.Structure determination indicated that **1**, **2** and **3**, respectively, possessed $[Fe_2S_2]^0$ core with $[Fe_2S_2]^0$-unit, $[Fe_3S_2]^0$ with $[Fe_2S_2]^{2-}$ and $[Fe_4S_2]^{2-}$ core with $[Fe_2S_2]^{4-}$ unit, which implied that $[Fe_2S_2(CO)_6]^{2-}$, as a starting material, underwent a disproportionation in the synthetic reaction.Investigating the structure and synthetic reaction, an origin of the different valence$[Fe_2S_2]$-units and formation pathways of those clusters via disproportionation of the $[Fe_2S_2(CO)_6]^{2-}$ following by 'Unit Construction' were proposed and discussed.

Keywords: Fe–S complex; $[Fe_2S_2]$-unit; Synthesis and structure; Formation pathway

1. Introduction

The chemistry of $[Fe_2S_2(CO)_6]$ has greatly interested chemists and bio-inorganic chemists because the reaction with participation of $[Fe_2S_2(CO)_6]$ or $[Fe_2S_2(CO)_6]^{2-}$ results in a variety of mixed-metal and mixed valence cluster complexes containing different $[Fe_2S_2]$-units which are very useful for investigation on the active center in metal enzymes and synthesis of novel poly-nuclear metal cluster compounds which possess novel structural conformation and significant physical and chemical properties [1–14].

It has been found that the cluster complexes containing $[Fe_2S_2]$-units from the reaction involving $[Fe_2S_2(CO)_6]$ reagent may possess two type conformations of $[Fe_2S_2]$, Plane type, for example, in $[MFe_2S_2(CO)_8dtc]^-$ (M = Mo, W; dtc = S_2CNEt_2), [15] and butterfly type, for instance, in $[VFe_4S_4(CO)_{12}]$ [16], $[MoOFe_5S_6(CO)_{12}]^{2-}$ [3], and $[Cu_5Fe_6S_6(CO)_{18}(PPh_3)_2]^-$ [8], and the valence of Fe in their $[Fe_2S_2]$-units can be 0, +1 and +2. Herein is reported synthesis and structures of new Fe–S cluster complexes containing different valence $[Fe_2S_2]$-units, $[Fe_2S_2(CO)_4(PPh_3)_2]$ (**1**), $[Fe_3S_2(CO)_6(PPh_3)_3]$ (**2**) and $[Ph_4P]_2[Fe_4S_2(CO)_{10}]$ (**3**), which implies the existence of $[Fe_2S_2(CO)_6]^0$ and $[Fe_2S_2(CO)_6]^{4-}$ species in the reaction system involving $[Fe_2S_2(CO)_6]^{2-}$, the origin of the $\{Fe_2S_2\}$-unit in metal–$[Fe_2S_2(CO)_6]$ cluster and formation pathway of the complexes were discussed.

---

* Corresponding author. Tel.: +86-591-3792464; fax: +86-591-3714946.
E-mail address: zbt@fjirsm.ac.cn (B. Zhuang).

0022-328X/$ - see front matter © 2004 Elsevier B.V. All rights reserved.
doi:10.1016/j.jorganchem.2004.05.036

2. Results and discussion

2.1. Synthesis

New Fe–S cluster complexes containing different valence $[Fe_2S_2]$-units, $[Fe_2S_2(CO)_4(PPh_2)_2]$ (**1**), $[Fe_3S_2(CO)_6(PPh_3)_3]$ (**2**) and $[Ph_4P]_2[Fe_4S_2(CO)_{10}]$ (**3**) were synthesized by the reaction of $[Fe_2S_2(CO)_6]$ with $LiEt_3BH$ in the presence of $CuCl\cdot PPh_3$, $AgNO_3–PPh_3$ and $CuClO_3\cdot MeCN$, respectively. Complex **2** also was prepared by reaction of $[Fe_2S_2(CO)_6]$ with $LiEt_3BH$ in the presence of PPh_3.

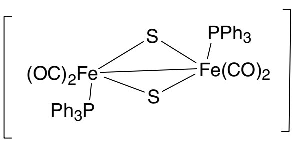

(1)

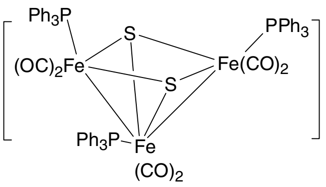

(2)

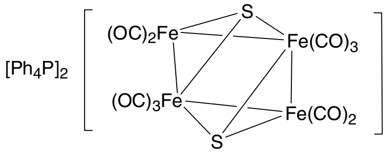

(3)

It is remarkable that complexes **1**, **2** and **3** do not possess any other metal atoms but iron atoms. This implies that the synthetic reaction of complexes **1**, **2** and **3** does not have the participation of CuCl, $AgNO_3$ and $CuClO_3$. The formation pathways of these complexes will be discussed later.

2.2. The crystal structure of $[Fe_2S_2(CO)_4(PPh_3)_2]$ (1)

The selected bond distances and bond angles of complex **1** are listed in Table 1 and the molecular structure of complex **1** was depicted in Fig. 1. As shown in Table 1 and Fig. 1, complex **1** contains a 'butterfly' type $[Fe_2S_2]^0$ core with Fe^{II}. Around each iron of the core there are two carbonyls and a PPh_3- ligand resulting in six coordination of the iron atom if considering the Fe–Fe bonding. Fe–Fe bond length is 2.5374(8) Å indicating the interaction between Fe and Fe atoms. Fe–S bond distances are 2.275(1), 2.275(1), 2.271(1) and 2.272(1) Å. The dihedral angle between the plane Fe1S2Fe2 and Fe1S1Fe2 is 74.42° indicating that the core $[Fe_2S_2]$ is in butterfly type configuration. Evidently, complex **1** should come from a $[Fe^{II}{}_2S_2(CO)_6]^0$-specie which undergoes substitution of carbonyl by PPh_3-ligand. Thus, the isolation of complex **1** strongly verified the existence of the species $[Fe^{II}{}_2S_2(CO)_6]^0$ which results from disproportionation of $[Fe_2S_2(CO)_6]^{2-}$ [15] in the synthetic reaction system.

Table 1
Selected bond distances (Å) and bond angles (°) of complex **1**

Bond distances			
Fe(1)–C(1)	1.754(5)	Fe(2)–P(2)	2.244 (1)
Fe(1)–C(2)	1.758(5)	Fe(2)–S(1)	2.272(1)
Fe(1)–P(1)	2.247(1)	Fe(2)–S(2)	2.271(1)
Fe(1)–S(1)	2.275 (1)	C(1)–O(1)	1.149(6)
Fe(1)–S(2)	2.275 (1)	C(2)–O(2)	1.150(6)
Fe(1)–Fe(2)	2.5374(8)	C(3)–O(3)	1.130(6)
Fe(2)–C(3)	1.762(5)	C(4)–O(4)	1.144(6)
Fe(2)–C(4)	1.768(5)		
Bond angles			
C(1)–Fe(1)–C(2)	92.6(2)	C(3)–Fe(2)–S(2)	87.0(2)
C(1)–Fe(1)–P(1)	96.9(2)	C(4)–Fe(2)–S(2)	157.9(2)
C(2)–Fe(1)–P(1)	100.6(2)	P(2)–Fe(2)–S(2)	102.45(5)
C(1)–Fe(1)–S(2)	87.2(2)	C(3)–Fe(2)–S(1)	160.0(2)
C(2)–Fe(1)–S(2)	155.7(2)	C(4)–Fe(2)–S(1)	92.7(2)
P(1)–Fe(1)–S(2)	103.51(4)	P(2)–Fe(2)–S(1)	98.62(5)
C(1)–Fe(1)–S(1)	161.9(2)	Fe(2)–S(1)–Fe(1)	67.83(4)
C(2)–Fe(1)–S(1)	90.6(2)	Fe(2)–S(2)–Fe(1)	67.86(4)
P(1)–Fe(1)–S(1)	100.03(4)	S(2)–Fe(2)–S(1)	82.81(5)
S(2)–Fe(1)–S(1)	82.66(5)	C(3)–Fe(2)–Fe(1)	104.0(2)
C(1)–Fe(1)–Fe(2)	105.9(2)	C(4)–Fe(2)–Fe(1)	103.5(2)
C(2)–Fe(1)–Fe(2)	101.0(2)	P(1)–Fe(2)–Fe(1)	146.04(4)
P(1)–Fe(1)–Fe(2)	147.57(4)	S(2)–Fe(2)–Fe(1)	56.14(3)
S(2)–Fe(1)–Fe(2)	56.00(3)	S(1)–Fe(2)–Fe(1)	56.15(3)
S(1)–Fe(1)–Fe(2)	56.02(3)	O(1)–C(1)–Fe(1)	179.3(5)
C(3)–Fe(2)–C(4)	90.3(2)	O(2)–C(2)–Fe(1)	177.8(4)
C(3)–Fe(2)–P(2)	100.4(2)	O(3)–C(3)–Fe(2)	179.0(4)
C(4)–Fe(2)–P(2)	99.6(2)	O(4)–C(4)–Fe(2)	178.6(5)

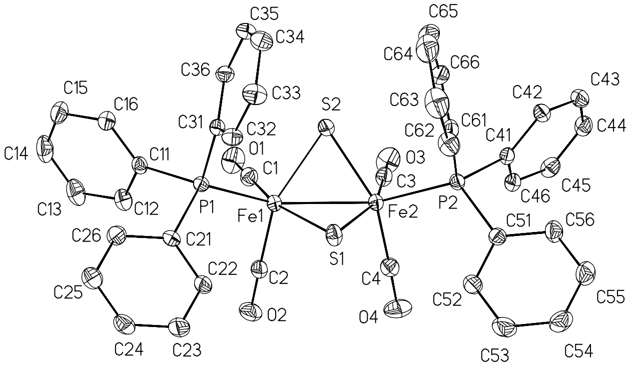

Fig. 1. The structure of compound $[Fe_2S_2(CO)_4(PPh_3)_2]$ (**1**).

2.3. The structure of $[Fe_3S_2(CO)_6(PPh_3)_3]$ (2)

In the crystals of complex **2**, $[Fe_3S_2(CO)_6(PPh_3)_3]$ complexes and H_2O molecules salvation are present. Selected bond distances and bond angles of complex **2** are listed in Table 2 and the molecular structure of complex **2** is de picted in Fig. 2. As is shown in Table 2 and Fig. 2, complex **2**, $[Fe_3S_2(CO)_6(PPh_3)_3]$, contains a distorted squre-pyramid $[Fe_3S_2]$-core with a pseudo-planar

Table 2
Selected bond distances (Å) and bond angles (°) of complex **2**·1/2H_2O

Bond distances			
Fe(1)–C(2)	1.771(6)	Fe(3)–C(6)	1.763(6)
Fe(1)–C(1)	1.785(6)	Fe(3)–C(5)	1.794(6)
Fe(1)–P(1)	2.245(1)	Fe(3)–P(3)	2.233(1)
Fe(1)–S(1)	2.261(2)	Fe(3)–S(1)	2.246(1)
Fe(1)–S(2)	2.266(1)	Fe(3)–S(2)	2.256(2)
Fe(1)–Fe(2)	2.608(1)	O(1)–C(1)	1.129(6)
Fe(1)–Fe(3)	2.653(1)	O(2)–C(2)	1.153(7)
Fe(2)–C(4)	1.750(6)	O(3)–C(3)	1.159(7)
Fe(2)–C(3)	1.769(6)	O(4)–C(4)	1.151(6)
Fe(2)–S(2)	2.231(1)	O(5)–C(5)	1.135(6)
Fe(2)–S(1)	2.274(2)	O(6)–C(6)	1.151(6)
Fe(2)–P(2)	2.281(2)		
Bond angles			
C(2)–Fe(1)–C(1)	99.6(3)	C(4)–Fe(2)–Fe(1)	149.5(2)
C(2)–Fe(1)–P(1)	89.1(2)	C(3)–Fe(2)–Fe(1)	100.1(2)
C(1)–Fe(1)–P(1)	91.9(2)	S(2)–Fe(2)–Fe(1)	55.18(4)
C(2)–Fe(1)–S(1)	111.9(2)	S(1)–Fe(2)–Fe(1)	54.67(4)
C(1)–Fe(1)–S(1)	147.8(2)	P(2)–Fe(2)–Fe(1)	113.65(5)
P(1)–Fe(1)–S(1)	95.37(5)	C(6)–Fe(3)–C(5)	92.8(2)
C(2)–Fe(1)–S(2)	109.4(2)	C(6)–Fe(3)–P(3)	94.0(2)
C(1)–Fe(1)–S(2)	85.3(2)	C(5)–Fe(3)–P(3)	92.7(2)
P(1)–Fe(1)–S(2)	161.49(6)	C(6)–Fe(3)–S(1)	149.7(2)
S(1)–Fe(1)–S(2)	77.96(5)	C(5)–Fe(3)–S(1)	88.0(2)
C(2)–Fe(1)–Fe(2)	75.3(2)	P(3)–Fe(3)–S(1)	116.21(6)
C(1)–Fe(1)–Fe(2)	131.7(2)	C(6)–Fe(3)–S(2)	96.5(2)
P(1)–Fe(1)–Fe(2)	135.10(5)	C(5)–Fe(3)–S(2)	165.7(2)
S(1)–Fe(1)–Fe(2)	55.14(4)	P(3)–Fe(3)–S(2)	97.56(5)
S(2)–Fe(1)–Fe(2)	53.93(4)	S(1)–Fe(3)–S(2)	78.48(5)
C(2)–Fe(1)–Fe(3)	157.5(2)	C(6)–Fe(3)–Fe(1)	98.5(2)
C(1)–Fe(1)–Fe(3)	94.2(2)	C(5)–Fe(3)–Fe(1)	113.6(2)
P(1)–Fe(1)–Fe(3)	108.26(5)	P(3)–Fe(3)–Fe(1)	150.14(5)
S(1)–Fe(1)–Fe(3)	53.68(4)	S(1)–Fe(3)–Fe(1)	54.20(4)
S(2)–Fe(1)–Fe(3)	53.89(4)	S(2)–Fe(3)–Fe(1)	54.24(4)
Fe(2)–Fe(1)–Fe(3)	82.25(3)	Fe(3)–S(1)–Fe(1)	72.12(5)
C(4)–Fe(2)–C(3)	94.5(3)	Fe(3)–S(1)–Fe(2)	99.90(5)
C(4)–Fe(2)–S(2)	110.4(2)	Fe(1)–S(1)–Fe(2)	70.20(5)
C(3)–Fe(2)–S(2)	154.4(2)	Fe(2)–S(2)–Fe(3)	100.95(6)
C(4)–Fe(2)–S(1)	98.3(2)	Fe(2)–S(2)–Fe(1)	70.90(4)
C(3)–Fe(2)–S(1)	92.5(2)	Fe(3)–S(2)–Fe(1)	71.87(4)
S(2)–Fe(2)–S(1)	78.40(5)	O(1)–C(1)–Fe(1)	178.0(5)
C(4)–Fe(2)–P(2)	90.6(2)	O(2)–C(2)–Fe(1)	173.3(5)
C(3)–Fe(2)–P(2)	97.3(2)	O(3)–C(3)–Fe(2)	173.3(7)
S(2)–Fe(2)–P(2)	88.58(5)	O(4)–C(4)–Fe(2)	174.9(5)
S(1)–Fe(2)–P(2)	166.14(6)	O(5)–C(5)–Fe(3)	177.0(5)
		O(6)–C(6)–Fe(3)	177.1(5)

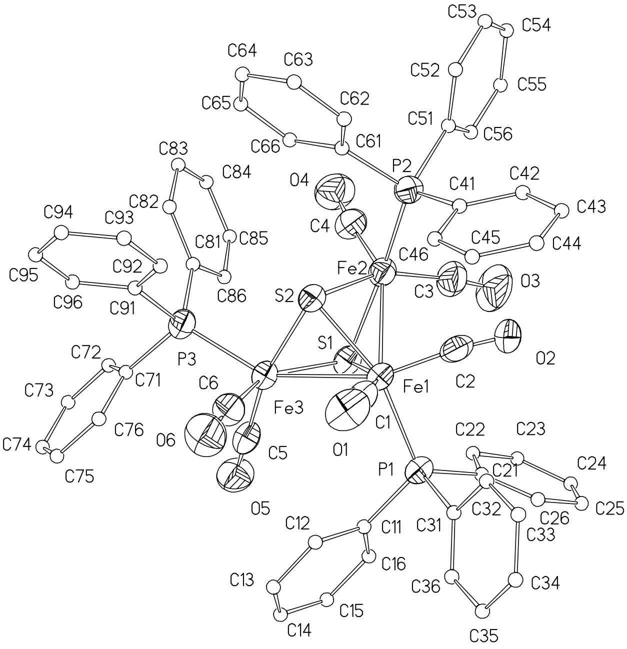

Fig. 2. The structure of compound $[Fe_3S_2(CO)_6(PPh_3)_3]$ (**2**).

$Fe(2)S(1)Fe(3)S(2)$ rhombus with dihedral angle of 17.7° as the base and Fe(1) atom on the apex. In the base, the Fe–S bond distances are 2.231(2), 2.246(2), 2.256(2) and 2.274(2) Å, and the $Fe(2)\cdots Fe(3)$ bond distance is 3.460 Å indicating non-metal–metal bonding. In the rest, the Fe(1)–S(1) and Fe(1)–S(2) are 2.261(2) and 2.266(1) Å, respectively, and the Fe(1)–Fe(2) and Fe(1)–Fe(3) bond distances are 2.608(1) and 2.653(1) Å, respectively. The core structure also could be considered as two butterfly type $[Fe_2S_2]$-unit sharing three atoms (S(1), S(2) and Fe(1)). There are two terminal carbonyls and a PPh_3-ligand connecting to each iron atom of the core forming the iron atoms in seven coordination for Fe(1) and six coordination for Fe(2) and Fe(3) if considering the Fe–Fe bonding. It is worth pointing out that the two PPh_3 ligands on the Fe atoms of the base in complex **2** adopted equatorial-axial coordination mode which was the same as that observed in $[Fe_3Te_2(CO)_7(PPh_3)_2$ [17], $[Ru_3Te_2(CO)_6(PPh_3)_3]$ [18] and $Fe_3S_2(CO)_7(PiPr_3)_2$ [19] and different from the equatorial-equatorial coordination scheme observed in selenido-analog $[Fe_3Se_2(CO)_7(PPh_3)_2]$ [20]. Complex **2** contains 50 skeleton electrons and possesses two Fe–Fe bonds indicating that its structure precisely obeys the $2(9N-L)$ (N = number of metal atoms and L = number of metal–metal bonds)rule [21]. To our knowledge, the iron–chalcogen–carbonyl analogs reported so far, for example, $[Fe_3S_2(CO)_9]$ [22], $[Fe_3Se_2(CO)_9]$ [23], $[Fe_3Te_2(CO)_9]$ [24], $[Fe_3S_2(CO)_8\ PCl_2SPh]$ [25], $[Fe_3S_2(CO)_8PPh_3]$ [26], $[Fe_3Te_2(CO)_9\ (PPh_3)]$ [24b], $[Fe_3S_2(CO)_8P(SPh_3)]$ [27], $[Fe_3S_2\ (CO)_7(Pi\ Pr_3)_2]$ [19], $[Fe_3Se_2(CO)_7(PPh_2C_2H_4\ PPh_2)]$ [28], $[Fe_3Se_2(CO)_7(PPh_3)_2]$ [20] and $[Fe_3Te_2(CO)_7(PPh_3)_2]$ [17] are unsubstituted, mono-substituted and di-substituted cluster complexes, trisubstituted one like complex **2** containing three substituting PPh_3-ligands has not been seen in the literature.

A butterfly type $[Fe_2S_2]$-unit with Fe–Fe bond of 2.60 Å and Fe–S of 2.57 Å comparable with the $[Fe_2S_2]^{2-}$-unit of $[Fe_2S_2(CO)_6]$ (Fe–Fe, 2.59 Å and Fe–S, 2.28 Å) [1,2] in complex **2**.

2.4. The structure of $[Ph_4P]_2[Fe_4S_2(CO)_{10}]$ (3)

Selected bond distances and bond angles of compound **3** are listed in Table 3 and the molecular structure of the anion of compound **3** is depicted in Fig. 3.

Table 3
Selected bond distances (Å) and bond angles (°) of complex **3**

Bond distances			
Fe(1)–C(1)	1.756(4)	Fe(2)–S#	2.173(1)
Fe(1)–C(2)	1.764(4)	Fe(2)–Fe(1)#	2.6121(6)
Fe(1)–S#	2.213(1)	S–Fe(2)#	2.173(1)
Fe(1)–S	2.213(1)	S–Fe(1)#	2.213(1)
Fe(1)–Fe(1)#	2.5250(9)	C(1)–O(1)	1.160(5)
Fe(1)–Fe(2)	2.6075(6)	C(2)–O(2)	1.160(5)
Fe(1)–Fe(2)#	2.6121(6)	C(3)–O(3)	1.147(5)
Fe(2)–C(4)	1.771(4)	C(4)–O(4)	1.145(4)
Fe(2)–C(5)	1.784(4)	C(5)–O(5)	1.138(4)
Fe(2)–C(3)	1.792(4)		
Bond angles			
C(1)–Fe(1)–C(2)	93.8(2)	C(4)–Fe(2)–C(5)	99.4(2)
C(1)–Fe(1)–S#	99.6(2)	C(4)–Fe(2)–C(3)	98.5(2)
C(2)–Fe(1)–S#	125.6(1)	C(5)–Fe(2)–C(3)	100.3(2)
C(1)–Fe(1)–S	128.0(1)	C(4)–Fe(2)–S#	103.2(1)
C(2)–Fe(1)–S	101.2(1)	C(5)–Fe(2)–S#	99.8(1)
S#–Fe(1)–S	110.42(3)	C(3)–Fe(2)–S#	147.4(1)
C(1)–Fe(1)–Fe(1)#	133.3(2)	C(4)–Fe(2)–Fe(1)	99.4(1)
C(2)–Fe(1)–Fe(1)#	132.9(2)	C(5)–Fe(2)–Fe(1)	150.9(1)
S#–Fe(1)–Fe(1)#	55.23(3)	C(3)–Fe(2)–Fe(1)	98.6(1)
S–Fe(1)–Fe(1)#	55.21(3)	S#–Fe(2)–Fe(1)	54.23(3)
C(1)–Fe(1)–Fe(2)	138.3(1)	C(4)–Fe(2)–Fe(1)#	153.8(1)
C(2)–Fe(1)–Fe(2)	83.3(1)	C(5)–Fe(2)–Fe(1)#	97.7(1)
S#–Fe(1)–Fe(2)	52.81(3)	C(3)–Fe(2)–Fe(1)#	97.8(1)
S–Fe(1)–Fe(2)	93.10(3)	S#–Fe(2)–Fe(1)#	53.16(3)
Fe(1)#–Fe(1)–Fe(2)	61.16(2)	Fe(1)–Fe(2)–Fe(1)#	57.86(3)
C(1)–Fe(1)–Fe(2)#	85.3(1)	Fe(2)#–S–Fe(1)#	72.96(3)
C(2)–Fe(1)–Fe(2)#	140.8(1)	O(2)–C(2)–Fe(1)	176.0(4)
S#–Fe(1)–Fe(2)#	92.98(4)	O(3)–C(3)–Fe(2)	178.6(4)
S–Fe(1)–Fe(2)#	52.73(3)	O(4)–C(4)–Fe(2)	179.5(4)
Fe(1)–Fe(1)–Fe(2)#	60.98(3)	O(5)–C(5)–Fe(2)	178.3(3)
Fe(2)–Fe(1)–Fe(2)#	122.14(2)		

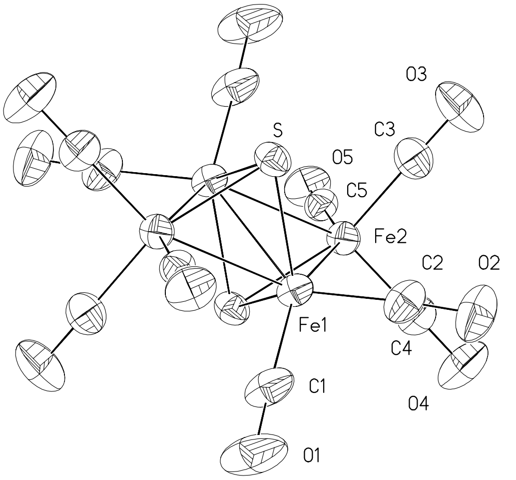

Fig. 3. The structure of the anion of compound $[Ph_4P]_2[Fe_4S_2(CO)_{10}]$ (**3**).

Compound **3** comprises two cations, $[Ph_4P]^+$, and a dianion $[Fe_4S_2(CO)_{10}]^{2-}$. As shown in Table 3 and Fig. 3, the anion of compound **3** possesses a $[Fe_4S_2]^{2-}$ core which consists of bi-distorted tetrahedron sharing an edge (Fe(1)–Fe(1)#) in *trans* arrangement. It can be found that there are two rhombic planes, Fe(1)–S–Fe(1)#–S#, with Fe–S bond distance of 2.213(1) Å and Fe–Fe bond length of 2.5250(9) Å and Fe(1)–Fe(2)–Fe(1)#–Fe(2)# with Fe–Fe bond lengths of 2.6075(6) and 2.6121(6) Å. The dihedral angle between this two planes is 62.71°. Each Fe atom in Fe(1)–S–Fe(1)#–S# plane is coordinated by two carbonyl groups resulting in seven coordination geometry including three Fe–Fe bonding. Each of the rest Fe atoms is connected with three carbonyl ligands resulting in six coordination geometry including two Fe–Fe bonding. Two sulfur atoms are μ_3-S and all carbonyls are terminal carbonyls. The fact that two kinds of iron atoms in different coordinating environments and two different Fe–S bond distances (2.213 and 2.173 Å) exist in compound **3** implies that there are two kinds of oxidation states for the iron atoms in compound **3**. According to the electric charge balance of the compound **3**, the oxidation states of the Fe atoms with longer Fe–S bond length (2.213 Å) in Fe(1)–S–Fe(1)–S# plane are zero and the rest Fe atoms with shorter Fe–S bond distances (2.173 Å) at both sides of Fe(1)–S–Fe(1)#–S# plane are +1. The skeleton electron number of compound **3** is 62 and five Fe–Fe bonds were observed in **3**. This shows that structure of **3** complied with the $2(9N-L)$ (N = number of metal atoms and L = number of metal–metal bonds) rule [21]. Complex **3** is a novel cluster compound completely different from the reported neutral iron–chalcogen–carbonyl tetra-nuclear cluster, $[Fe_4(CO)_{10}(\mu_4\text{-E})_2(\mu\text{-CO})]$ (E = S [29], Se [30] and Te [31], which consists of a planar arrangement of four iron atoms with quadruply bridging S (or Se or Te) atoms on each side of the Fe_4-unit, a bridging carbonyl and two semi-bridging carbonyls.

It is worth noting that a new $[Fe_2S_2]$-unit with Fe^0, $[Fe_2S_2]^{4-}$, is found in compound **3** and this may evidence the existence of an another species, $[Fe_2S_2(CO)_6]^{4-}$, which results from the disproportionation of $[Fe_2S_2(CO)_6]^{2-}$ [15] in the synthetic reaction system.

2.5. $Fe_2S_2]^0$-, $[Fe_2S_2]^{2-}$-, $[Fe_2S_2]^{4-}$-units and disproportionation of $[Fe_2S_2(CO)_6]^{2-}$

Summarizing the structures of complex **1**, **2** and **3** mentioned above, there exist three kinds of $[Fe_2S_2]$-units, $[Fe_2S_2]^0$ with Fe^{II} atoms in compound **1**, $[Fe_2S_2]^{2-}$ with Fe^{I} atoms in compound **2** and $[Fe_2S_2]^{4-}$ with Fe^0 atoms in compound **3**, and several kinds of $[Fe(CO)_{3-n}L_n]^{z+}$ (L = PPh_3, $n = 1$, $z = 2$ (in **2**); $n = 0$, $z = 1$ (in **3**)) fragments in these complexes. Noteworthily, the structures of complexes **1**, **2** and **3** do not have any other metal atom but iron atoms although their syntheses were carried out in the presence of CuCl or $CuClO_4$ or $AgNO_3$. This indicates that the formation of complexes **1**, **2** and **3** only result from a change of the $[Fe_2S_2(CO)_6]^{2-}$ itself, which is derived from the reaction of $[Fe_2S_2(CO)_6]$ with reduction reagent $LiEt_3BH$. [2] In fact, compound **2** can also be obtained from the synthetic reaction without $AgNO_3$ (see Section 3.3b).

Taking account into the three oxidation states of $[Fe_2S_2]$-units, $[Fe_2S_2]^0$, $[Fe_2S_2]^{2-}$ and $[Fe_2S_2]^{4-}$, observed in compound **1**, **2** and **3**, it is undoubted that in the synthetic reaction system, there should exist three diiron-disulfide carbonyl species, $[Fe_2S_2(CO)_6]^0$, $[Fe_2S_2(CO)_6]^{2-}$ and $[Fe_2S_2(CO)_6]^{4-}$, which are able to generate the $[Fe_2S_2]^0$, $[Fe_2S_2]^{2-}$ and $[Fe_2S_2]^{4-}$-units and provide the iron carbonyl fragments, $[Fe(CO)_3]^+$, $[Fe(CO)_3]^{2+}$ and $[Fe(CO)_3]^0$, when they undergo decomposition. Interestingly, the three species, $[Fe_2S_2(CO)_6]^0$, $[Fe_2S_2(CO)_6]^{2-}$ and $[Fe_2S_2(CO)_6]^{4-}$, are just the disproportionation products of $[Fe_2S_2(CO)_6]^{2-}$. Therefore, the isolation of the complexes **1** with $[Fe_2S_2]^0$, **2** with $[Fe_2S_2]^{2-}$ and **3** with $[Fe_2S_2]^4$-units evidences that the disproportionation reaction of $[Fe_2S_2(CO)_6]^{2-}$ and the decomposition of the disproportionation products $[Fe_2S_2(CO)_6]^{0,\ 2-,\ 4-}$ occur in the reaction system involving the reagent $[Fe_2S_2(CO)_6]^{2-}$.

It is apparent that the $[Fe_2S_2]$-units in M–$[Fe_2S_2(CO)_6]$ cluster complexes should result from the products of the disproportionation of $[Fe_2S_2(CO)_6]^{2-}$ and the M–$[Fe_2S_2(CO)_6]$ cluster complexes may form via unit construction of the species from disproportionation of $[Fe_2S_2(CO)_6]^{2-}$ and metal compound including iron carbonyl fragments from decomposition of the disproportionation products. Thus, in the synthetic reaction system involving with $Fe_2S_2(CO)_6$ reagent, the self-change of $[Fe_2S_2(CO)_6]$ and formation of M–$[Fe_2S_2(CO)_6]$-cluster compounds via an unit construction of reactive fragment or species can be described as following Scheme 1.

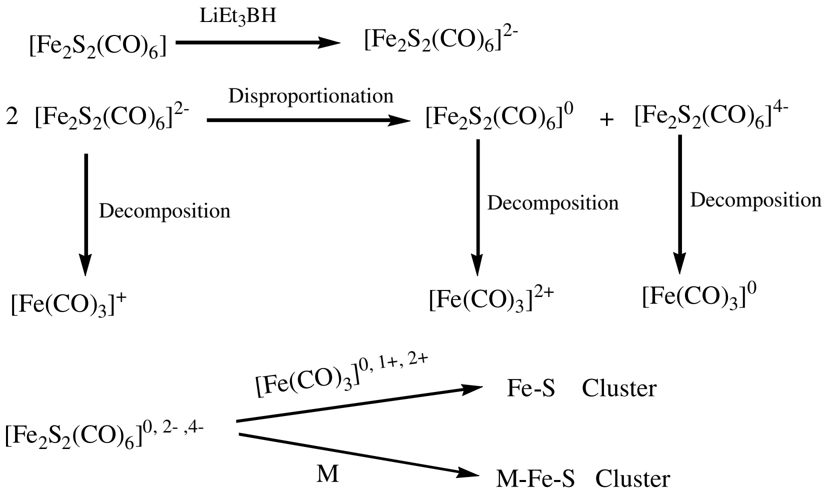

Scheme 1.

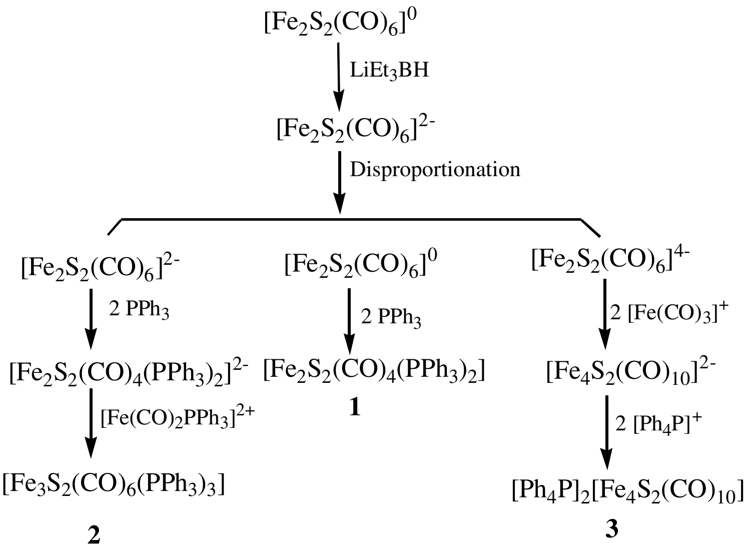

Scheme 2.

*2.6. Formation pathways of complexes **1**, **2** and **3***

As is discussed above, the synthetic reaction and formation pathways of complexes **1**, **2** and **3** could be figured out in Scheme 2 and more clearly described as Figs. 4–6. As is shown in Scheme 2, in the synthetic reaction system, the starting material $[Fe_2S_2(CO)_6]$ was reduced to its di-anion $[Fe_2S_2(CO)_6]^{2-}$ by reducing reagent $LiEt_3BH$ and this di-anion underwent disproportionation resulting in three species, $[Fe_2S_2(CO)_6]^0$, $[Fe_2S_2(CO)_6]^{2-}$ and $[Fe_2S_2(CO)_6]^{4-}$.

Two PPh_3-ligand replace the carbonyls of the neutral species $[Fe_2S_2(CO)_6]^0$ containing Fe^{II} to obtain compound **1** (Fig. 4) and the $[Fe_2S_2]^0$ in compound **1** came from the $[Fe_2S_2(CO)_6]^0$ species. Like compound **1**, the di-anionic species $[Fe_2S_2(CO)_6]^{2-}$ reacts with PPh_3 to

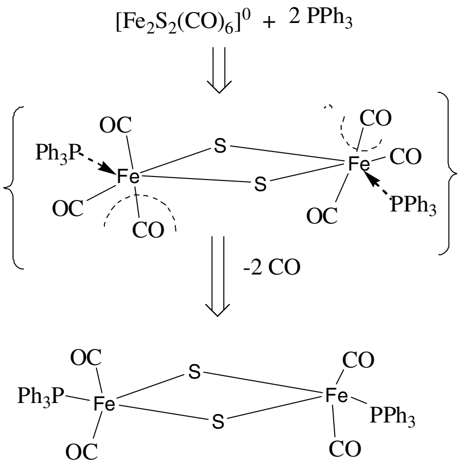

(1)

Fig. 4. Formation pathway of compound **1**.

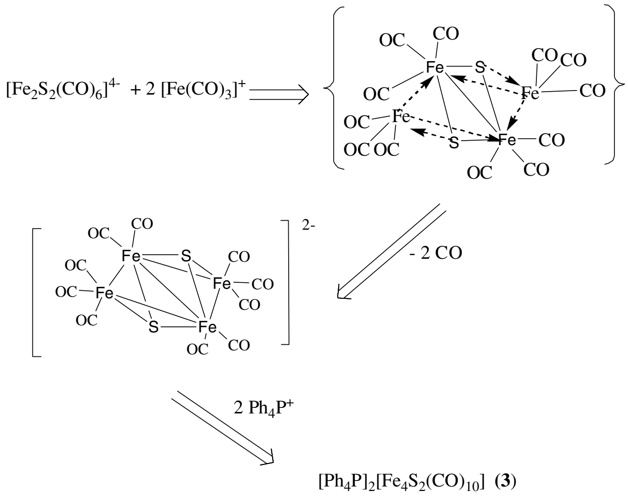

Fig. 6. Formation pathway of compound **3**.

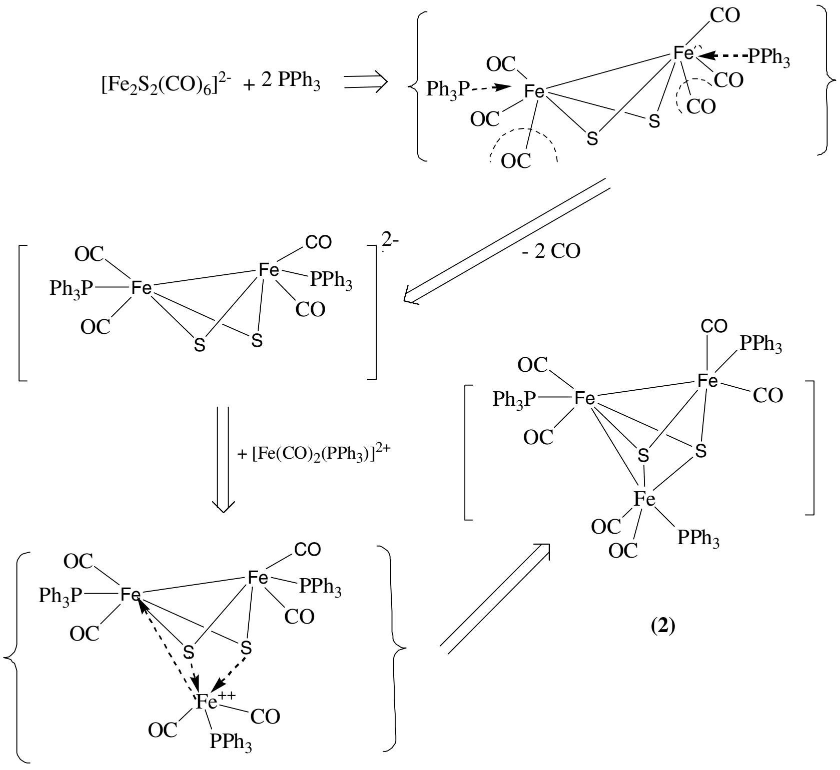

Fig. 5. Formation pathway of compound **2**.

give a PPh_3-substituting Fe^I–S–CO compound with butterfly type $[Fe_2S_2]^{2-}$-unit, $[Fe_2S_2(CO)_4(PPh_3)_2]^{2-}$, and when the $[Fe_2S_2(CO)_4(PPh_3)_2]^{2-}$ further reacts with PPh_3-substituting iron-carbonyl fragment $[Fe(CO)_2PPh_3]^{2+}$, the lone pair electrons on the S atoms of $[Fe_2S_2(CO)_4(PPh_3)_2]^{2-}$ coordinated to the Fe atom of $[Fe(CO)_2PPh_3]^{2+}$ accompanied with establishment of a Fe–Fe bond between the Fe atom of $[Fe(CO)_2PPh_3]^{2+}$ and one of the Fe atoms of $[Fe_2S_2(CO)_4(PPh_3)_2]^{2-}$ affording tri-nuclear cluster $[Fe_3S_2(CO)_6(PPh_3)_3]$ (**2**). (Fig. 4) The butterfly type $[Fe_2S_2]^{2-}$-unit in compound **2** is obviously derived from the di-anionic species $[Fe_2S_2(CO)_6]^{2-}$ and the pseudo plane $[Fe_2S_2]$-unit without Fe–Fe bonding in **2** took shape after the reaction of $[Fe_2S_2(CO)_4(PPh_3)_2]^{2-}$ with $[Fe(CO)_2PPh_3]^{2+}$. When the tetra-anionic species $[Fe_2S_2(CO)_6]^{4-}$ reacted with $[Fe(CO)_3]^+$ fragments, two S atoms of the tetra-anionic species $[Fe_2S_2(CO)_6]^{4-}$, respectively, coordinated to the Fe atoms of two $[Fe(CO)_3]^+$ fragments from both sides of the planar $[Fe_2S_2]$-unit of the tetra-anionic species $[Fe_2S_2(CO)_6]^{4-}$ accompanied with creation of four Fe–Fe bonds between the Fe atom of tetra-anionic species $[Fe_2S_2(CO)_6]^{4-}$ and the Fe atom of $[Fe(CO)_3]^+$ fragments resulting in tetra-nuclear cluster $[Fe_4S_2(CO)_{10}]^{2-}$ which was collected as Ph_4P^+-salt, $[Ph_4P]_2[Fe_4S_2(CO)_{10}]$ (**3**). (Fig. 6) It is evident that the $[Fe_2S_2]^{4-}$-unit came from the tetra-anionic species $[Fe_2S_2(CO)_6]^{4-}$.

It must be pointed out that there are other possible formation pathways for complex **2**: an unsubstituted $[Fe_2S_2(CO)_6]^{2-}$ species reacts with $[Fe(CO)_3]^{2+}$ fragment to form $[Fe_3S_2(CO)_9]$ cluster compound which undergoes PPh_3-substitution resulting in complex **2** or a $[Fe_4S_2(CO)_{11}]$, generated from the reaction system, reacts with PPh_3 to give complex **2** like Ru-analog $[Ru_3S_2(CO)_6(PPh_3)_3]$ [18], but taking notice of the fact that no $[Fe_3S_2(CO)_9]$, $[Fe_4S_2(CO)_{11}]$, $[Fe_3S_2(CO)_8PPh_3]$ and $[Fe_3S_2(CO)_7(PPh_3)_2]$ have been isolated from the synthetic reaction system of complex **2**, these two formation pathways for complex **2** may be excluded.

Finally, it should be pointed out that the Cu(Ag)–$[Fe_2S_2(CO)_6]$ complexes have not been isolated although the synthetic reactions were carried out in the presence of Cu^+ and Ag^+. This is due to the larger electronegativities of Cu (1.9)and Ag (1.9) than Fe (1.8) [32], thus, the Cu^+ and Ag^+ are less positive than Fe^+ or Fe^{++}, and the negative species $[Fe_2S_2(CO)_6]^{n-}$ ($n = 0$, 2 and 4) tend to react with Fe^+ or Fe^{++}. As a matter of fact, the M–$[Fe_2S_2(CO)_6]$ complexes (M=Mo^0 [15], Mo^v [3], W^0 [15], V^{VI} [16], Mn^{II} [16], Cr^{II} [16],) have been obtained because the electronegativities of Mo, W, V, Mn and Cr are less than or equal to that of Fe. So, it will be possible to obtain a new Metal–$[Fe_2S_2(CO)_6]$ cluster compound if the metal ion with less electronegativity than Fe^+ or Fe^{++} and proper reaction condition such as reactant ratio, precipitate reagent, reaction temperature and so on are used. In fact, a Fe^{III}–$[Fe_2S_2(CO)_6]$ compound $[Fe_6S_6(CO)_{12}]^{2-}$ [33] was collected beside the compound **3** in the synthetic reaction of compound **3**. $[Fe_6S_6(CO)_{12}]^{2-}$ possesses a $[Fe_2S_2]^{2+}$-unit with Fe^{III}, which is more positive than Fe^+. The negative $[Fe_2S_2(CO)_6]^{2-}$ species tend to react with $[Fe_2S_2]^{2+}$-unit resulting in $[Fe_6S_6(CO)_{12}]^{2-}$ (see Section 3.4) The $[Fe_2S_2]^{2+}$-unit may be derived from a species, $[Fe_2S_2\text{- }(CO)_6]^{2+}$, which might be a oxidation product of $[Fe_2S_2\text{- }(CO)_6]^0$ by ClO_4^-.

3. Experimental

3.1. Materials and methods

CH_3CN, CH_2Cl_2 and THF were distilled with CaH_2, P_2O_5 and $LiAlH_4$, respectively, CH_3OH and ^iPrOH were dried by distillation with $Mg(OMe)_2$. PPh_3, $Fe(CO)_5$ and $LiEt_3BH$ in THF were purchased from Fluka. CuCl and $AgNO_3$were products of Shanghai Chemical Company. $[Fe_2S_2(CO)_6]$ were prepared by reaction of $Fe(CO)_5$ with Na_2S_5 and KOH in MeOH [1,2].

IR spectra were recorded on Nicolet Magno 750 and elemental analysis were performed on Carlo Erba Instrumentation Elemental Analyzer-MOD 1106.

All reaction procedures were carried out under N_2 atmosphere by using Schlenk technique and all solvents and reagents were degassed before use.

3.2. Synthesis of $[Fe_2S_2(CO)_4(PPh_3)_2]$ (*1*)

To a red solution of $[Fe_2S_2(CO)_6]$ (0.25 g, 0.73 mmol) in 20 ml THF was dropped slowly 1.5 ml 1 M $LiEt_3BH$–THF at −78 °C under stirring resulting in green solution, and, then, to this green solution was added a mixture of CuCl (0.072 g, 0.72 mmol), PPh_3 (0.38 g, 1.45 mmol) and Et_4NCl (0.12 g, 0.73 mmol) in 20 ml MeCN. After the temperature rose to room temperature by removing the cold-bath, the reaction mixture was stirred at room temperature for 24 h. Filtering off small amount of solid, the brown filtrate was concentrated to 15 ml, and 8 ml of isopropanol was added. After filtering off a small amount of precipitate again, the resulting filtrate was cooled at 4 °C for three months. 0.13 g of red brown crystalline $[Fe_2S_2(CO)_4(PPh_3)_2]$ (**1**) was obtained by filtration, washed with isopropanol and dried in vacuum. Yield: 21.9% (base on $[Fe_2S_2(CO)_6]$ used). Anal. Calc. for $C_{40}H_{30}Fe_2O_4P_2S_2$: C, 59.1; H, 3.7; P, 7.6; Fe, 13.8. Found: C, 58.9; H, 3.4; P, 7.2; Fe, 13.5%. IR (KBr pellet): 1994, 1952, 1932, 1909 cm^{-1} (ν_{CO}).

3.3. Synthesis of $[Fe_3(CO)_6(PPh_3)_3]$ (*2*)

(a) To a red solution of $[Fe_2S_2(CO)_6]$ (0.25 g, 0.73 mmol) in 20 ml THF was dropped 1.5 ml 1M $LiEt_3BH$ in THF at −78 °C under stirring resulting in a green solution and then $AgNO_3(PPh_3)_2$ (0.5 g, 0.61 mmol) in 20 ml MeCN was added into this green solution. After the temperature rose to room temperature by removing the cold bath, the resulting reaction mixture was stirred at room temperature overnight, 0.12 g (0.73 mmol) of Et_4NCL was added and the reaction mixture was stirred for another 16 h resulting in brown solution with some solid in it. After filtering off small amount of solid, the brown filtrate was concentrated to dryness. The residue was dissolved in 20 ml MeCN and 9 ml isopropanol was added. Filtering off a little bit precipitate, the filtrate was cooled at 4 °C for a month. 0.2 g of crystalline $[Fe_3S_2(CO)_6(PPh_3)_3]$ (**2**) was collected by filtration, washed with isopropanol and dried in vacuum. Yield: 34% (based on $[Fe_2S_2(CO)_6]$ used) Anal. Calc. for $C_{60}H_{45}Fe_3O_6P_3S_2$: C, 60.7; H, 3.8; Fe, 14.2; S, 5.4; P, 7.8. Found: C, 59.8; H, 3.9; Fe, 13.8; S, 5.3; P, 7.4%. IR (KBr pellet): 1996, 1973, 1954, 1934, 1911, 1900 cm^{-1} (ν_{CO}).

(b) To the solution of $[Fe_2S_2(CO)_6]$ (0.3 g, 0.87 mmol) in 25 ml THF was dropped slowly 1.8 ml 1 M $LiEt_3BH$ in THF at −78 °C under stirring resulting in green solution and PPh_3 (0.48 g, 1.83 mmol) in 70 ml MeCN was added. After the reaction temperature was raised to room temperature by removing cold bath, the reaction mixture was stirred at room temperature for 24 h resulting in green solution. After filtering (no precipitate was found), the green filtrate was concentrated to dryness by vacuum and the residue was dissolved in 15 ml MeCN and then 8 ml isopropanol was added. After filtering, the resulting filtrate was cooled at 4 °C for several months crystalline **2** was obtained.

3.4. Synthesis of $[Ph_4P]_2[Fe_4S_2(CO)_{10}]$ (3)

To a red solution of $[Fe_2S_2(CO)_6]$ (0.25 g, 0.73 mmol) in 20 ml THF was dropped slowly 1.5 ml 1M $LiEt_3BH$ in THF at −78 °C under stirring and then a solution of $CuClO_4 \cdot MeCN$ (0.15 g, 0.73 mmol) in 20 ml CH_3CN was added. After removing cold bath, the reaction temperature rose to room temperature and the reaction mixture was stirred at room temperature for 3 h. Ph_4PBr (0.3 g, 0.72 mmol) was added and the resulting mixture was continued to stir overnight. After filtering off a small amount of black precipitate, the brown filtrate was concentrated to dryness. The residue was dissolved in 25 ml CH_2Cl_2, and after filtering off some gray solid the brown filtrate was concentrated again to dryness. The residue was dissolved in 17 ml CH_3CN and 8 ml isopropanol was added. After filtering, the filtrate was cooled at 4 °C for more than two months. 0.1 g crystalline $[Ph_4P]_2[Fe_4S_2(CO)_{10}]$

Table 4
Crystal data and collection and refinement details for **1**, **2**·H_2O and **3**

Compounds	**1**	**2**·H_2O	**3**
Empirical formula	$C_{40}H_{30}Fe_2O_4P_2S_2$	$C_{60}H_{46}Fe_3O_{6.5}P_3S_2$	$C_{29}H_{20}Fe_2O_5PS$
Formula weight	812.40	1195.55	623.18
Temperature (K)	293	293	293
Crystal system	Monoclinic	Monoclinic	Monoclinic
Space group	$P2_1/n$	$P2_1/n$	$P2_1/n$
Unit cell dimensions			
a (Å)	10.2905(2)	17.262(3)	10.8238(2)
b (Å)	22.411(4)	14.985(4)	14.8907(1)
c (Å)	17.1882(3)	21.442(4)	17.2887(3)
α (°)	90	90	90
β (°)	96.265(1)	96.67(1)	90.4460(1)
γ (°)	90	90	90
V (Å^3)	3940.2(1)	5509(2)	2786.40(7)
Z	4	4	4
D_{calc} (mg cm^{-3})	1.369	1.442	1.486
λ (mm^{-1})	0.962	0.994	1.210
Crystal size (mm^3)	0.45×0.3×0.2	0.45×0.2×0.2	0.4×0.25×0.2
θ Range (°)	1.50–25.08	1.66–23.27	1.80–25.15
Index ranges	$-12 \leqslant h \leqslant 12$	$-19 \leqslant h \leqslant 17$	$-12 \leqslant h \leqslant 12$
	$-21 \leqslant k \leqslant 26$	$-12 \leqslant k \leqslant 16$	$-17 \leqslant k \leqslant 12$
	$-12 \leqslant l \leqslant 20$	$-22 \leqslant l \leqslant 23$	$-20 \leqslant l \leqslant 16$
Reflections collected	15,798	24,585	13,947
Independent reflections	6921	7849	4958
No. observations with $I > 2\sigma(I)$	5653	6455	4892
Data/restrains/parameters	6913/0/451	7849/0/671	4956/0/343
Goodness-of-fit	1.158	1.040	1.134
R_1, wR_2 ($I > 2\sigma(I)$)	0.0505, 0.1605	0.0512, 0.1346	0.0413, 0.1095
R_1, wR_2 ($I > 2\sigma$ (I)	0.0649, 0.1793	0.0660, 0.1475	0.0595, 0.1262
Largest difference peak and hole (e Å^{-3})	1.676/−0.440	1.291/−0.365	0.467/−0.756

(**3**) was collected by filtration, washed with isopropanol and dried in vacuum. Yield: 22% (based on $[Fe_2S_2(CO)_6]$ used). Anal. Calc. for $C_{29}H_{20}Fe_2O_5PS$: C, 55.8; H, 3.2; Fe, 18.0; P, 5.0; S, 5.1. Found: C, 55.2; H, 3.1; Fe, 17.6; P, 4.9; S, 5.0%. IR (KBr pellet): 1994, 1952, 1932, 1909 cm^{-1} (ν_{CO}).

The mother liquid was continued to stand at 4 °C for several days. A known product $[Ph_4P]_2[Fe_6S_6(CO)_{12}]$ [26] was obtained.

3.5. X-ray crystal structure determination

A crystal samples of compound **1**, **2**·1/2H_2O and **3** wrapped with glue were mounted on Siemems Smart CCD diffractometer equipped with a graphite monochromator (Mo Kα radiation $\lambda = 0.71073$ Å) for data collection. The crystal data, collection and refinement details are listed in Table 4. All calculations were performed on a Silicon Graphics computer station by using the SHELXTL program system.

Data were corrected for Lorentz and polarization effects and absorption effects by SADABS [34]. The structure was solved by directed methods (SHELXTL) and were refined by the full-matrix least-squares on all F^2 data using Silicon Graphics Indy computer [35].

4. Summary

New di-, tri- and tetra-nuclear Fe–S carbonyl complexes, $[Fe_2S_2(CO)_4(PPh_3)_2]$(**1**), $[Fe_3S_2(CO)_6(PPh_3)_3]$ (**2**), and $[Ph_4P]_2[Fe_4S_2(CO)_{10}]$ (**3**) have been isolated from the reaction involving with $[Fe_2S_2(CO)_6]$ and $[Fe_2S_2(CO)_6]^{2-}$. Crystal structure determination indicated that **1**, **2** and **3** contained $[Fe_2S_2]$ core with $[Fe_2S_2]^0$-unit, $[Fe_3S_2]$ core with $[Fe_2S_2]^{2-}$-unit and $[Fe_4S_2]^{2-}$ core with $[Fe_2S_2]^{4-}$-unit, respectively. These $[Fe_2S_2]$-units in different oxidation states observed in **1**, **2** and **3** correspond to that in the disproportionation products of $[Fe_2S_2(CO)_6]^{2-}$ and evidence that a disproportionation of $[Fe_2S_2(CO)_6]^{2-}$ occurs in the synthetic reaction system. The formation pathways of **1**, **2** and **3** via unit construction of disproportionation products of $[Fe_2S_2(CO)_6]^{2-}$ have been figured out and the origin of $[Fe_2S_2]$-units in M–$[Fe_2S_2(CO)_6]$ cluster has been discussed.

5. Supplementary material

Crystallographic data for the structural analysis have been deposited with the Cambridge Crystallographic Data Centre, CCDC nos. 197026, 197027 and 197028 for compounds **1**, **2**, and **3**, respectively. Copies of this information may be obtained free of charge from The Director, CCDC, 12, Union Road, Cambridge CB2 1EZ, UK (fax: +44-1233-336033; e-mail: deposit@ccdc.cam.ac.uk or www: http://www.ccdc.cam.ac.uk).

Acknowledgement

We are grateful to the National Natural Science Foundation of China and State Key Laboratory of Structural Chemistry for financial support in this research.

References

[1] D. Seyferth, R.S. Henderson, M.K. Gallagher, J. Organomet. Chem. 193 (1980) C75.

[2] D. Seyferth, R.S. Henderson, Li-Chen Song, Organometallics 1 (1982) 125.

[3] K.S. Bose, P.E. Lamberty, J.A. Kouacs, E. Sinn, B.A. Averill, Polyhedron 5 (1986) 393.

[4] P.A. Eldredge, R.F. Bryan, E. Sinn, B.A. Averill, J. Am. Chem. Soc. 110 (1988) 5573.

[5] K.S. Bose, S.A. Chmielewski, P.A. Eldredge, E. Sinn, B.A. Averill, J. Am. Chem. Soc. 11 (1989) 8953.

[6] P.A. Eldredge, K.S. Bose, D.E. Barber, B.A. Averill, Inorg. Chem. 30 (1991) 2365.

[7] D.E. Barber, R.F. Bryan, M. Sabat, K.S. Bose, B.A. Averill, Inorg. Chem. 35 (1996) 4635.

[8] B. Zhuang, B. Pan, L. Huang, P. Yu, Inorg. Chim. Acta 227 (1994) 119.

[9] P. Braunstein, J.-M. Jud, C.M. Tiripicchio, E. Bapa, Angew. Chem. Int. Ed. Engl. 21 (1982) 307.

[10] M.D. Curits, P.D. Williams, W.M. Butler, Inorg. Chem. 27 (1988) 2853.

[11] M. Cowie, R.L. Dekock, T.R. Wagenmaker, D. Seyferth, R.S. Henderson, M.K. Gallager, Organometallics 8 (1989) 119.

[12] N.S. Nametkin, V.D. Tyurin, M.A. Kukina, Russ. Chem. Rev. 55 (1986) 439.

[13] P. Mathur, D. Chakrataty, I.J. Mavunkal, J. Cluster Sci. 4 (1993) 351.

[14] F. Osterich, C. Achim, R.H. Holm, Inorg. Chem. 40 (2001) 224.

[15] B. Zhuang, P. Chen, L. Huang, Polyhedron 11 (1992) 127.

[16] B. Zhuang, J. Chen, L. He, H. Sun, Z. Zhou, K. Wu, Z. Huang, J. Organomet. Chem. 682 (2003) 59.

[17] A.L. Rheingold, R.L. Ostrander, P. Mathur, Acta Crystallogr. C49 (1993) 1741.

[18] P. Mathur, B.H.S. Thimmappa, A.L. Rheingold, Inorg. Chem. 29 (1990) 4658.

[19] I.L. Eremenko, S.E. Nefedov, D.A. Veghini, S. Rosenberger, H. Beke, L.A. Oishniskaya, V.M. Novotortsev, IZV. Akad. Nauk. SSSR, Ser Khim (1997) 141.

[20] P. Baistrocchi, D. Cauzzi, H. Lanfranchi, G. Predieri, A. Tiripicchio, M.I. Camellini, Inorg. Chim. Acta 235 (1995) 173.

[21] (a) A.Q. Tang, S.Q. Li, Kexue Tongbao 29 (1983) 1621;
(b) A.Q. Tang, S.Q. Li, Sci. Sinica (B) 31 (1988) 918.

[22] (a) C.H. Wei, L.F. Dahl, Inorg. Chem. 4 (1965) 493;
(b) R. Seidel, B. Schnautz, G. Henkel, Angew. Chem. Int. Ed. Engl. 35 (1996) 1710.

[23] R. Seidel, B. Schnautz, G. Henkel, Angew. Chem., Int. Ed. Engl. 35 (1996) 1710.

[24] (a) D.A. Lesch, T.B. Rauchfuss, Inorg. Chem. 20 (1981) 3583;
(b) D.A. Lesch, T.B. Rauchfuss, Organometallics 1 (1982) 499.

[25] Q. Liu, S. Liu, B. Wu, Q. Suo, X. Hu, B. Wang, Acta Phys. Chim. Sin. 6 (1990) 730.

[26] P. Baistrocchi, M. Careri, C. Graiff, M. Lanfranchi, P. Manini, G. Preddieri, A. Tripicchio, Inorg. Chim. Acta 252 (1996) 367.

[27] Q. Liu, B. Wu, X. Hu, S. Liu, X. Yan, J. Shi, Acta Chim. Sinica 50 (1992) 778.

[28] D. Cauzzi, C. Graiff, M. Lanfranchi, G. Predieri, A. Tripicchio, J. Organomet. Chem. 536 (1997) 497.

[29] R.D. Adams, J.E. Babin, J. Estrada, J.-G. Wang, Polyhedron 8 (1989) 1885.

[30] P. Mathur, Md.M. Hassain, R.S. Rashid, J. Organomet. Chem. 476 (1994) 245.

[31] T.F. Fässber, T. Vögl, P.B. Fabritchnyi, M.I. Afanasov, J. Organomet. Chem. 561 (1998) 221.

[32] E.G. Rochow, Organometallic Chemistry, Chapman & Hall, London, 1965 p. 6.

[33] G.L. Lilley, E. Sinn, B.A. Averill, Inorg. Chem. 25 (1986) 1073.

[34] G.M. Sheldrick, SADAS, Absorption Correction Program, University of Gottingen, 1996.

[35] G.M. Sheldrick, SHELXTL 5.03, Siemens Analytical X-ray Instrument Inc., Madison, WI, 1990.